EAI Endorsed Transactions
on Energy Web
Research Article EAI.EU

Digital Twin-Driven State Estimation and Control for EV Adjustable Capability under Constraint Drift

Qianru Zhao[1,*], Zeguang Shao[1], Shaoxiong Li[3], Chaoyang Li[2], Chun Li[4] and Lei Li[1]

[1]State Grid Tianjin Marketing Service Center, Tianjin
[2]State Grid Tianjin Jinghai Power Supply Co., Ltd., Tianjin
[3]State Grid Tianjin Binhai Company, Tianjin
[4]State Grid Tianjin Chengxi Electric Power Supply Branch, Tianjin

Abstract

With the rapid growth of electric vehicles (EVs), EV flexibility has become a key resource for enhancing distribution network resilience and facilitating renewable energy integration. However, the time-varying physical constraints of distribution networks, the dynamic response of electricity market incentives, and the uncertainty in EV user behavior make it difficult to accurately estimate adjustable capability in real time. To address this problem, this paper proposes a Digital Twin (DT)-driven state estimation and control framework for online state estimation of EV adjustable capability under constraint drift. First, a multi-dimensional physical model is established by coupling distribution-network security constraints, electricity-market incentive constraints, and EV operation constraints. Second, a digital twin historical scenario library is constructed to support scenario similarity matching, state-feature fusion, and drift-intensity quantification. Third, a hierarchical state-drift estimation method is designed to distinguish single-constraint drift from multi-constraint interactive drift. Finally, a twin-driven boundary evolution and distributed control execution strategy is developed by combining adaptive state estimation, two-stage warm start, and the alternating direction method of multipliers. Case studies based on charging-pile operational data in Tianjin show that the proposed method can dynamically track constraint drift, update EV adjustable boundaries, and provide high-precision state estimates for distribution-network dispatch.

Keywords: electric vehicles, digital twin, state estimation, adjustable capability

Received on 20 August 2026, accepted on 20 October 2026, published on 12 November 2026

Copyright © 2026 Qianru Zhao *et al.*, licensed to EAI. This is an open access article distributed under the terms of the CC BY-NC-SA 4.0, which permits copying, redistributing, remixing, transformation, and building upon the material in any medium so long as the original work is properly cited.

doi: 10.4108/ew.14638

1. Introduction

In the context of Industry 5.0 and the Industrial Internet of Things (IIoT), as the global energy structure transitions to clean, low-carbon energy, EVs have become the primary means to promote decarbonization and energy system upgrades in the transportation sector, given their zero-emission and high-efficiency technical advantages [1]. It is expected that the EV penetration rate may reach 80% by 2030 [2].

DT technology provides a new technical paradigm for real-time modeling, state perception, state estimation, prediction, and closed-loop control of complex energy systems [3-4]. In EV–distribution-network interaction scenarios, DT can synchronously map the operating states of distribution networks, electricity-market signals, EV charging/discharging behavior, and user-side response characteristics. Therefore, introducing a DT framework into EV adjustable capability state estimation transforms static

*Corresponding author. Email: cindyrqcz@gmail.com

boundary evaluation into dynamic state estimation and boundary evolution [5-7].

Regarding the impacts of EV integration on distribution networks and the evaluation of flexibility capabilities, a case study was conducted to examine the influence of EV charging, charging speed, and charging strategies on the distribution grid [8]. Residential charging flexibility boundaries were extracted and defined to support quantitative flexibility characterization [9]. Cross-system coordination between power distribution and traffic networks with EVs was addressed using an ALADIN-based method [10]. The hosting capacity of a low-voltage distribution network for EV adoption was evaluated, providing evidence for access-capability assessment [11].

Regarding EV adjustable capability evaluation conditions, a DC microgrid energy management strategy was proposed for workplace/building electric vehicle charging stations during grid outages [12]. A two-stage physical–economic adjustable-capacity evaluation model was proposed for EVs that provide peak-shaving and valley-filling auxiliary services [13]. An LSTM network–based charging management method was proposed, focusing on forecasting and scheduling non-critical charging sessions [14]. The uncertain scheduling potential of charging stations was analyzed under multi-attribute uncertain charging decisions, clarifying how uncertainty affects feasible scheduling boundaries [15].

More recently, drift-aware data-driven methods and Digital Twin technologies have been introduced into dynamic energy-management applications. A drift-aware approach to data-driven evolutionary computation was proposed [16]. A novel Digital Twin framework that integrates discrete-event simulation with a multi-objective optimization engine for intelligent electric vehicle charging is proposed [17]. A novel microgrid digital twin is proposed to optimize electric vehicle fleet charging schedules for maximum photovoltaic self-consumption [18]. A novel method that integrates reliability indicators, such as expected load loss and expected unserved energy, is proposed to simulate the stochastic characteristics of electric vehicle charging behavior [19]. The applications of digital technologies are comprehensively discussed, including artificial intelligence-based price prediction algorithms, digital twins, blockchain-powered energy trading markets, energy price fluctuation data analysis, as well as vehicle-to-grid technology and price stabilization mechanisms [20].

Although existing research has achieved advances in EV charging load analysis, boundary extraction, grid-EV coordination and adjustable capacity evaluation, three drawbacks persist: separate modeling of grid, market and EV constraints fails to reflect coupled EV adjustable boundaries; constraint dynamics are regarded as external disturbances, causing inaccurate lagging responses to constraint drift; digital twin historical data are merely offline samples instead of a DT scenario library for online estimation and control initialization.

To address these gaps, this paper presents a closed-loop DT-driven framework for estimating the adjustable capability state of EVs, develops a hierarchical twin-driven state-drift estimation method for single-constraint drift and multi-constraint interactive drift, and designs a DT boundary evolution and distributed control strategy integrating state feedback, scenario reuse, and two-stage warm-start optimization. The proposed method provides a model–data hybrid Digital Twin perception and control framework for EV adjustable capability estimation under dynamic constraint interactions.

For clarity and ease of reference, the main abbreviations and mathematical symbols repeatedly used in this paper are summarized in Table 1.

Table 1. Nomenclature and abbreviations used in the proposed framework

Symbol / Abbreviation	Definition
EV	Electric vehicle
DT	Digital Twin
SOC	State of charge
ADMM	Alternating Direction Method of Multipliers
KS	Kolmogorov–Smirnov test
AD	Anderson–Darling test
LSTM	Long Short-Term Memory
ALADIN	Augmented Lagrangian Alternating Direction Inexact Newton
DG	Distributed generation
S	Constraint-drift intensity
D_W	KS statistic between adjacent data windows
A^2	Anderson–Darling statistic between adjacent data windows
E_{online}	Online state-estimation error
ρ	ADMM penalty parameter
λ	Lagrange multiplier
P_{adj}	EV adjustable power
$P_{adj,true}$	Actual EV adjustable power
$Sim_{curr,hist}$	Similarity between the current DT state and a historical DT scenario
$MD_{curr,hist}$	Mapping distance between the current and historical DT states
$AE_{curr,hist}$	Approximation error between the current and historical scenarios

2. EV Model Construction

The collaborative hierarchical architecture in this chapter is shown in Figure 1 to adapt to dynamic constraint scenarios. The core participants in the architecture include distribution network operators, power market operators, EV aggregators, and EV users, forming a closed loop of multi-source data interactions among these entities.

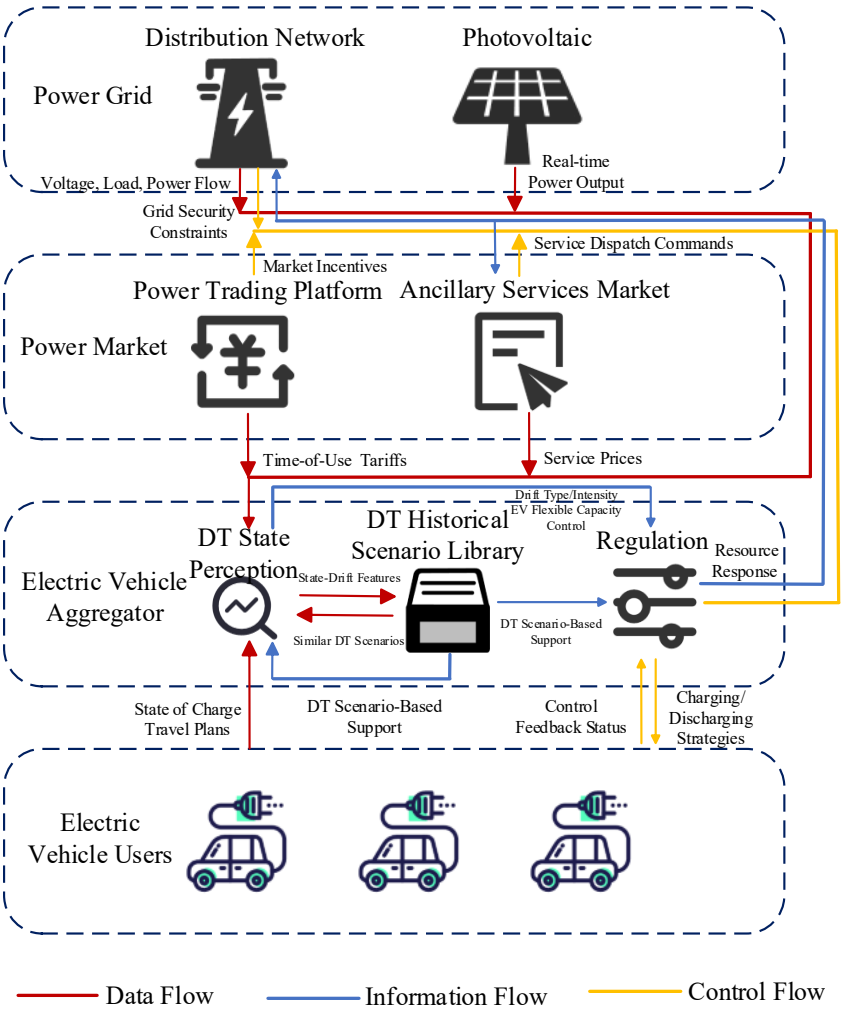


Figure 1. Digital Twin-driven hierarchical architecture for EV adjustable-capability state estimation and distributed control

Figure 1 illustrates how grid-state measurements, market information, EV operational states, historical DT scenarios, and control feedback are integrated into a closed-loop state-estimation and control framework.

2.1 Multi-dimensional Coupling Constraint Model

This section develops the EV–grid–market physical modeling module of the Digital Twin. The module couples distribution-network security constraints, electricity-market incentive constraints, and EV operation constraints into a unified state-estimation framework.

Grid constraints are the core physical boundaries to ensure the safe, high-quality, and economical operation of the distribution network. The spatiotemporal distribution characteristics of EV charging and discharging power directly affect the dynamic change of constraints.

The power market guides EV users to participate in grid dispatch through price signals and incentive mechanisms. To reduce the obstruction to photovoltaic power generation in the office area, EV users can reach the office area during the day and stay for extended periods, and formulate an EV charging pricing plan based on photovoltaic output in the office area.

The core premise of EV adjustable capability is that EVs themselves have the potential to adjust, and ignoring battery

characteristics will lead to estimated adjustable capabilities beyond the actual executable range of EVs.

2.2 Digital Twin Historical Scenario Library and Data Foundation

A digital twin historical scenario library is constructed for EV adjustable capability state estimation. The library stores digital twin historical operating states of the EV–grid–market system and provides the data foundation for scenario similarity matching, state-feature fusion, drift-intensity quantification, and control initialization. Each scenario record includes grid physical-state information, market-state information, EV operation-state information, and control-feedback information.

The similarity between the current twin state and the stored digital twin scenarios is quantified based on the mapping distance and approximate error, as shown in the following equation:

$$MD_{\text{curr,hist}} = \frac{1}{M}\sum_{i=1}^{M}(f_{\text{curr},i} - f_{\text{hist},i})^2 \tag{1}$$

$$AE_{\text{curr,hist}} = \frac{1}{N}\sum_{j=1}^{N}(\hat{P}_{\text{adj,hist},j} - P_{\text{adj,true},j})^2 \tag{2}$$

$$Sim_{\text{curr,hist}} = \frac{1}{MD_{\text{curr,hist}} + AE_{\text{curr,hist}} + \delta} \tag{3}$$

Where M is the number of core constraint features; $f_{\text{curr},i}$ and $f_{\text{hist},i}$ are the eigenvalues of the current twin state and digital twin scenario, respectively; N is the number of EV samples in the digital twin scenario; $P_{\text{adj,true},j}$ is the real adjustable power.

To quantify drift intensity, a moving window is adopted to characterize the time-varying distribution of the core features. The window size is set to 50 to ensure statistical reliability.

Three-level confidence levels are set up, corresponding to the warning interval coefficients k_1=1, k_2=2, k_3=3. The characteristic deviation is correlated with the confidence interval to quantify the drift intensity S, and the confidence level weight is introduced to highlight the influence of high confidence drift:

$$S = \sum_{i=1}^{3}\omega_{L_i}\cdot\frac{\hat{\mu} + k_i\cdot\hat{\sigma} - \mu_{\text{norm}}}{\sigma_{\text{norm}}} \tag{4}$$

where μ_{norm} and σ_{norm} are the mean and standard deviation of the digital twin historical normal state distribution of the feature, respectively.

Then calculate the final fusion weight:

$$\omega_{\text{fusion},k} = \eta'_k\cdot(0.6\cdot\frac{S_k+\varepsilon}{\sum S_j+\varepsilon} + 0.4\cdot\max_{\text{hist}\in Arc_EV} Sim_{\text{curr,his}}\cdot\omega_{\text{hist},k}) \tag{5}$$

Where $\omega_{\text{hist},k}$ is the weight of the k-type constraint in a similar digital twin scenario.

3. Twin-Driven State Perception and State-Drift Estimation

EV state drift refers to the deviation of key twin-state features from the digital twin historical normal operating state of the EV–grid–market system. These features include grid physical-state variables, market incentive-state variables, and EV operation-state variables. State drift directly affects the digital twin adjustable boundary and the executable control capability of EV clusters.

To address real-time state estimation under dynamic constraint interactions, this section develops an adaptive segmentation and hierarchical state-drift estimation method based on twin-state features.

3.1 Adaptive Segmentation and State-Feature Extraction

Given the different drift patterns of physical-state and market-state variables, grid physical-state drift is usually abrupt and requires high temporal resolution, whereas market-state drift is generally gradual and does not require excessively frequent sampling. A fixed segmentation strategy may miss abrupt physical-state drift or introduce redundant data during gradual market-state changes. Therefore, an adaptive segmentation method is developed to adjust the temporal resolution of the Digital Twin according to the fluctuation intensity of state features.

Based on the difference in drift characteristics between physical and economic constraints, a drift-sensitive adaptive segmentation method is proposed.

Firstly, the original fluctuation coefficient of the feature is calculated based on the sliding window, and the dynamic change degree of the feature is quantified:

$$F_0(t) = \frac{\sigma_{\text{win}}(t)}{\mu_{\text{win}}(t)} \tag{6}$$

where $F_0(t)$ is the original fluctuation coefficient; $\sigma_{\text{win}}(t)$ is the standard deviation of the features in the sliding window; $\mu_{\text{win}}(t)$ is the mean value of the features in the window.

The physical constraint drift is mostly manifested as a mutation in the characteristic distribution, and the statistic D_W of the KS test is used as the correction term to quantify the difference in the distribution:

$$F_{\text{phys}}(t) = F_0(t) \times (1 + k \cdot D_W) \tag{7}$$

where k is the correction coefficient, D_W is the KS test statistic of the t window and the previous window, and the feature distribution in the two windows is checked.

The economic constraint drift is mostly manifested as a sudden change in the characteristic variance, and the statistic A^2 of the AD test is used as the correction term:

$$F_{\text{econ}}(t) = F_0(t) \times (1 + m \times \frac{A^2}{3}) \tag{8}$$

where m is the correction coefficient, and A^2 is the AD test statistic of the window and the previous window.

Based on the optimized volatility coefficient, the segment interval can be dynamically adjusted, which can effectively track the period of high volatility and reduce the degree of data redundancy, as shown in Table 1.

Table 2. Volatility coefficient rules

Coefficient fluctuation range	Segmented intervals	Applicable scenarios
$F(t) \le 0.3$	30min	Stable constraint
$0.3 < F(t) \le 0.6$	15min	Slow changes in constraints
$F(t) > 0.6$	5min	Constraints on rapid drift

The thresholds in Table 2 are empirical segmentation cutoffs. They are determined from the distribution of the optimized fluctuation coefficient F(t) in the Digital Twin historical scenario library and are used to distinguish stable, slowly varying, and rapidly drifting operating regimes. The numerical cutoffs are therefore dataset-calibrated operating thresholds and can be re-identified when the historical scenario library is updated [16].

Based on the original sampling data on the physical constraints of the power grid, the economic constraints of the electricity market, and the constraints of the EV itself, four types of statistics are extracted through adaptive segmentation, and a 36-dimensional structured feature vector is ultimately formed. The eigenvector is output as a row vector, expressed as:

$$X(t) = \left[\hat{x}_1, \sigma_1, k_1, c_1; \ldots; \hat{x}_9, \sigma_9, k_9, c_9\right] \tag{9}$$

This subsection realizes the transformation from adaptive segmentation data quantification to a feature vector by clarifying the prerequisites for feature extraction. The output 36-dimensional eigenvector contains the baseline level, fluctuation degree, change trend, and sudden change of constraints.

3.2 Hierarchical State-Drift Estimation

Hierarchical state-drift estimation is designed to identify whether the current twin state is affected by single-constraint drift or multi-constraint interactive drift. The first layer estimates single-constraint drift by comparing the current state-feature vector with the digital twin historical normal state interval. The second layer evaluates interactive drift by measuring the coupling relationship among different constraint states using Pearson correlation and mutual information. This structure improves the accuracy and timeliness of state estimation under multi-constraint interactions.

Assuming that the mean value of the grid voltage deviation in digital twin historical data is $\mu\Delta U$ and the standard deviation is $\sigma\Delta U$, the normal interval of voltage deviation can be expressed as:

$$\Delta U_{\text{normal}}(t) = \left[\mu\Delta U - k \cdot \sigma\Delta U,\ \ \mu\Delta U + k \cdot \sigma\Delta U\right] \tag{10}$$

To avoid misjudgement caused by a single statistic anomaly, the rules of multi-feature coordination and time continuity should be adopted, as follows. For a certain type of constraint (such as the physical constraint of the power grid), at least 2 characteristics must exceed its digital twin historical normal range and contain at least 1 core feature, and the core feature is the key index of the constraint, such as the core feature of the physical constraints of the power grid is voltage deviation and load factor; The core characteristics of market constraints are the electricity price fluctuation coefficient and auxiliary service income. The core characteristics of EV's own constraints are the SOC change rate and travel time deviation.

The second layer addresses scenarios where multiple single-constraint drifts occur simultaneously. Its objective is to distinguish interactive drift from parallel drift. A two-index collaborative verification method is adopted, combining the Pearson correlation coefficient for linear correlation and the mutual information for nonlinear correlation, given by:

$$r = \frac{\sum_{i=1}^{M}(x_i - \bar{x})(y_i - \bar{y})}{\sqrt{\sum_{i=1}^{M}(x_i - \bar{x})^2} \times \sqrt{\sum_{i=1}^{M}(y_i - \bar{y})^2}} \tag{11}$$

$$MI(X,Y) = \sum_{x \in X}\sum_{y \in Y} p(x,y) \ln \frac{p(x,y)}{p(x)p(y)} \tag{12}$$

where x_i and y_i are the feature statistics of constraints A and B, respectively; M is the number of digital twin

historical segments used to calculate the correlation; X and Y are the feature statistic sequences of constraint A and constraint B, respectively.

When the system detects that two or more constraint types are marked as a single independent drift in a continuous period of time, the interactive drift decision is automatically triggered. For any two different types of constraints in the set, if at least one pair of constraints satisfies the condition: $|r| \geq \theta_{\text{lin}}$ or $MI \geq \theta_{\text{nonlin}}$, the current scene is determined to be a multi-constraint interaction drift.

3.3 Digital Twin Boundary Evolution and Adaptive State Estimation

The digital twin boundary evolution mechanism supports the dynamic adaptation of EV adjustable capability under state drift. Once the twin-driven state perception module identifies state drift, the Digital Twin updates the adjustable boundary of EV clusters according to the estimated drift type, drift intensity, confidence level, and online estimation error. The adjustable boundary is modeled as a dynamically evolving state variable, driven by real-time measurements, digital twin historical scenario knowledge from the digital twin, and control-feedback information.

$$C_k^{'} = C_k \begin{cases} 1-0.2\text{II} & (h_{L3} \geq mh_{L3}) \quad (L3\ Hit) \\ 1-0.1\text{II} & (h_{L2} \geq mh_{L2}) \quad (L2\ Hit) \\ 1 & (No\ Hit) \end{cases} \tag{13}$$

where C_k is the original constraint boundary.

The state estimation frequency adjustment is based on the two-index collaborative judgment of online error and drift intensity, balancing real-time performance and computational overhead. The online error is as follows:

$$E_{\text{online}} = \frac{1}{I}\sum_{\text{i=1}}^{I}(\hat{P}_{\text{adj},i} - P_{\text{adj,true},i})^2 \leq 0.05 \tag{14}$$

where I is the number of iterations; $P_{\text{adj,true},i}$ is the actual value.

Quantify the current adaptation accuracy, and the drift intensity S quantifies the environment's dynamics; the two jointly determine the state estimation frequency. The specific adjustment rules and visualizations are as follows

(i) Strong dynamic environment: $E_{\text{online}} > 0.1$ or $S \geq 1.2$, fast tracking of environmental changes;
(ii) Medium dynamic environment: $0.05 < E_{\text{online}} \leq 0.1$ or $0.5 \leq S < 1.2$, balance response and overhead;
(iii) Stable environment: $E_{\text{online}} \leq 0.05$ or $S < 0.5$, reducing computing consumption.

The update of Arc_{EV} is follows the two principles of accuracy and reusable scenes to ensure the validity and timeliness of digital twin historical scenario knowledge.

Current twin-state information may be stored in the database. The threshold is set because when the online error exceeds 0.05, the deviation between the state-estimation result and the actual adjustable capability is large, and reusing such information will introduce initialization errors in the two-stage bipolar warm-start, reducing optimization accuracy.

4. Model solution

The distributed control execution module generates charging and discharging strategies for EV aggregators and EV users based on the estimated digital-twin-adjustable boundary. A two-layer control model is constructed to coordinate grid-side global control and user-side individual decision-making. The upper layer minimizes network loss and voltage deviation while maximizing EV adjustable potential, and the lower layer maximizes user charging and discharging benefits while satisfying SOC, travel demand, and node-level adjustable-boundary constraints.

The Alternating Direction Method of Multipliers (ADMM) is a distributed optimization method that decomposes a coupled optimization problem into several smaller subproblems and coordinates them through augmented-Lagrangian multipliers and consistency constraints. It combines the decomposability of dual methods with the convergence characteristics of augmented-Lagrangian optimization, making it suitable for problems involving multiple decision-making entities and coupled boundary variables.

The ADMM algorithm is used to realize distributed control execution and closed-loop coordination between grid-side and user-side decisions.

(iv) Upper layer: the global optimisation layer dominated by grid constraints

This layer is dominated by grid constraints. The objective is to minimize grid loss and voltage deviation while maximizing the adjustable potential of EVs, integrating network loss models with digital twin historically similar environments to improve computational efficiency:

$$\min F_{\text{upper}} = \omega_1 \cdot \frac{P_{\text{loss}}}{P_{\text{loss,max}}} + \omega_2 \cdot \frac{\Delta U_{\text{avg}}}{\Delta U_{\text{max}}} - \omega_3 \cdot \frac{P_{\text{adj,total}}}{P_{\text{total,max}}} \tag{15}$$

The weights ω_1, ω_2, and ω_3 are determined by scene similarity and fusion weights.

(v) Lower layer: user decision-making layer dominated by market constraints

This layer is dominated by market constraints. The goal is to maximise user charging and discharging benefits and reuse

optimal digital twin historical strategies. The objective function is:

$$\max F_{\text{lower},i} = R_{\text{as},i}(t) - C_{\text{charge},i}(t) - C_{\text{loss},i}(t) \quad (16)$$

where the income from auxiliary services, charging cost, and battery loss cost are considered. The EV's own constraints and the upper global power boundary are included as follows:

$$\begin{cases} SOC_i^{\min} \le SOC_i(t) \le SOC_i^{\max} \\ SOC_i(t_{\text{depart}}) \ge SOC_i^{\min,\text{depart}} \\ -P_{\text{ev},i}^{\max,\text{discharge}} \le P_{\text{ev},i}(t) \le P_{\text{ev},i}^{\max,\text{charge}} \\ \sum_{i\in\Omega_j} P_{\text{ev},i}(t) \le P_{\text{adj},j}(t) \end{cases} \quad (17)$$

To address the coupling characteristics between the two-layer model of global grid optimization and individual user decision-making, and the real-time requirements of online state estimation, the Alternating Direction Method of Multipliers (ADMM) is used to implement a distributed optimization solution. The distributed control execution flowchart is shown in Figure 2. The flowchart shows that historical DT scenarios provide the initial operating point, while ADMM iteratively coordinates grid-level adjustable-boundary estimation and user-level charging/discharging decisions until convergence is achieved.

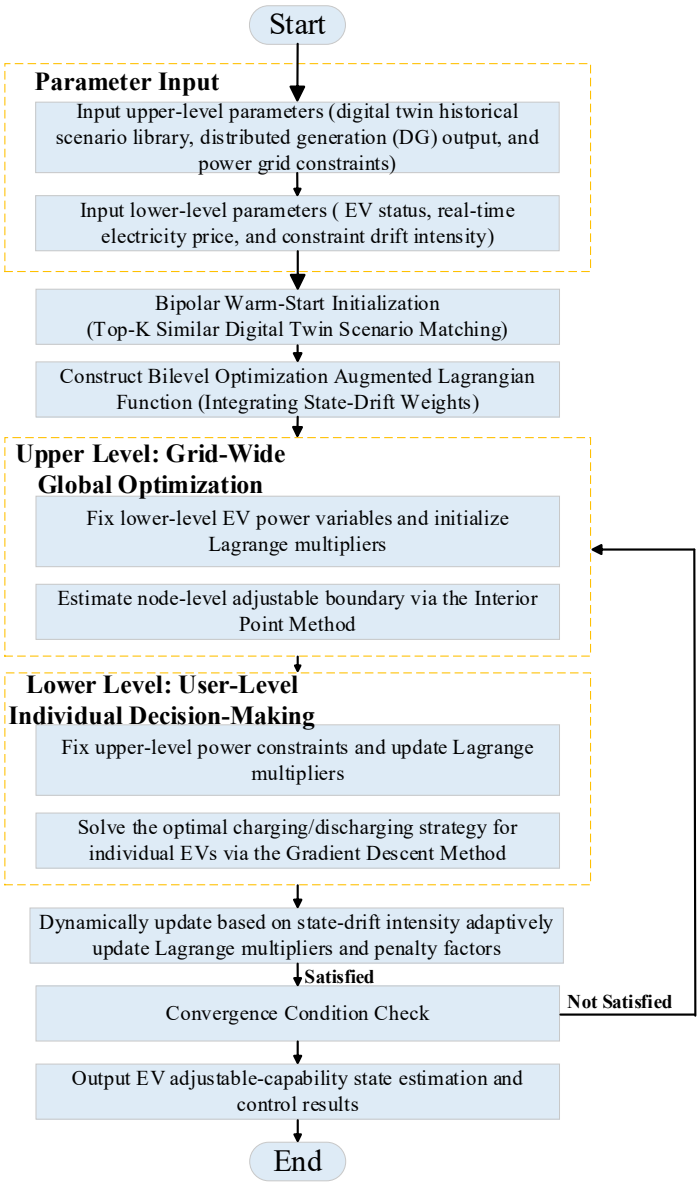


Figure 2. Distributed control execution process integrating DT scenario-based warm-start initialization and ADMM-based coordination between grid-level and EV-level optimization

The specific steps are:

(i) Input the $top-K$ similar scene parameters, two-layer optimization model constraints, constrained drift intensity, and fusion weights of the digital twin historical scenario library, perform two-level bipolar warm-start initialization, and construct the augmented Lagrangian function of the two-layer coupling problem;
(ii) The global optimization sub-problem of the upper-layer power grid is solved by fixing the individual charging and discharging power variables of the lower EV users and the current Lagrangian multiplier, and the optimal solution of the node-level adjustable power upper limit of the distribution network is obtained by using the internal point method;
(iii) Fixed upper power grid nodes, adjustable power constraint variables, and updated Lagrangian multipliers, distributed according to nodes to solve individual decision sub-problems of lower users, and reused the digital twin historical optimal strategy to obtain the optimal strategy for charging and discharging a single EV through the gradient descent method;
(iv) Based on the iterative results of the upper and lower layer sub-problems and the constraint drift intensity, the Lagrangian multiplier and penalty factor are adaptively updated, and the change rate of the consistency constraint residual and the objective function value is calculated;
(v) Check whether the convergence conditions are met, and if they are not met, return to step 2 to continue iteration; if they are met, the final state-estimation results of EV adjustable capabilities, such as node-level adjustable power and user-level charging and discharging strategy, are output, and the solution is completed.

For reproducibility, the initial ADMM penalty parameter is set to $\rho_0 = 1.0$. The algorithm is considered converged when both the normalized consistency residual and the relative variation of the augmented objective function satisfy the prescribed tolerances. Specifically, the consistency-residual tolerance is set to $\varepsilon_{\text{conv}} = 5\times10^{-4}$ while the relative objective-function variation is required to be no greater than 10^{-5} for two consecutive iterations. In addition, the multiplier-update step is adaptively adjusted according to the state-drift intensity. When $S \geqslant 1.2$, the update step is increased by 20% to improve the tracking speed under strongly dynamic conditions; when $S < 0.5$, the update step is reduced by 10% to suppress oscillation under relatively stable conditions.

To prevent excessive computation in exceptional non-convergent cases, a maximum iteration number of $N_{\max} = 100$ is adopted. If the convergence criteria are not satisfied within $N_{\max}$iterations, the iterative procedure is terminated and the current solution is flagged as non-converged.

The distributed solution strategy based on two-stage bipolar warm-start and ADMM proposed in this chapter can effectively solve the strong coupling problem of the two-layer optimization model and the real-time bottleneck in dynamic drift scenarios. Through the dual-level bipolar warm-start, information from similar digital twin scenes is fully reused, significantly reducing the initial deviation and the computational overhead of model iteration. Relying on the ADMM distributed decoupling iteration and an adaptive multiplier and penalty factor adjustment mechanism, the solution accuracy and convergence speed in complex drift scenarios are considered, and efficient coordination between the overall optimization of the power grid and the individual decision-making of users is achieved.

5. Case Study

This section uses operation data of charging piles in a certain area of Tianjin, covering two typical scenarios of office areas and residential areas, including node voltage, distribution network load rate, real-time electricity price, EV charging and discharging power, SOC changes, etc.

The dynamic synergy characteristics among adjustable power, electricity price, and the remaining state of charge of EVs are shown in Figure 3. When the SOC is in the range of 0.4 - 0.8, the adjustable power is maintained in the range of 0.5-1.25kW, and the trend increases with increasing SOC because the battery charge and discharge adjustment space is larger at high SOC. When the real-time electricity price is lower than 0.35 yuan/kWh (valley period), the adjustable power is significantly increased, peaking at 1.25kW, while the electricity price is higher than 0.6 yuan/kWh (peak time). The adjustable power is reduced to less than 0.25kW, which verifies the incentive and constraint effect of electricity price on adjustable capacity. The synergistic effect between electricity price and SOC is evident: the adjustable potential is largest in high-SOC, low-electricity-price scenarios and smallest in low-SOC, high-electricity-price scenarios.

It should be noted that Figure 3 combines representative samples from both office-area and residential-area scenarios to characterize their common SOC–electricity-price–adjustable-power coupling rather than to provide a direct regional comparison. Nevertheless, the two scenarios exhibit different temporal availability characteristics. Office-area EVs generally arrive during daytime and remain parked for relatively long periods, resulting in a longer daytime regulation window and greater responsiveness to daytime electricity-price and renewable-energy variations.

In contrast, residential-area charging is mainly concentrated after users return home, so its adjustable capability is shifted toward the evening and nighttime periods and is more strongly constrained by the required departure SOC and subsequent travel demand. Therefore, the regional difference mainly affects the time and duration for which EV flexibility is available, whereas the fundamental coupling between SOC, electricity price, and adjustable power shown in Figure 3 is observed in both scenarios.

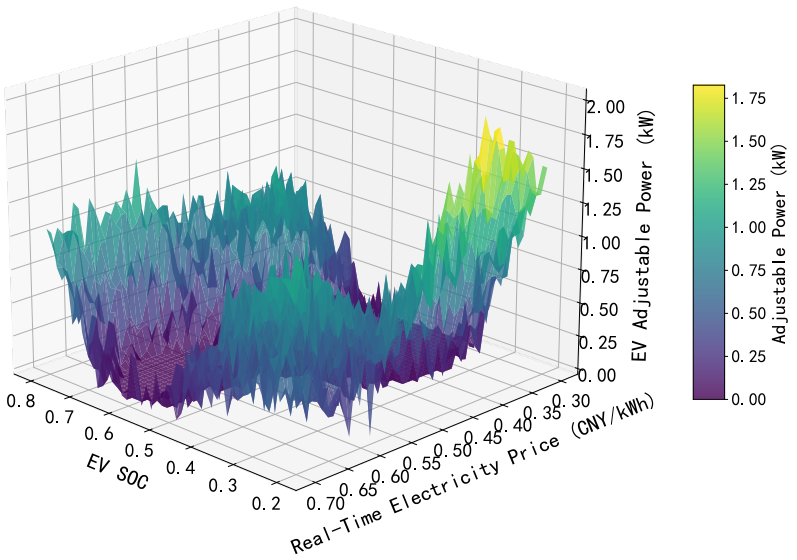


Figure 3. Coupled relationship among EV adjustable power, electricity price, and SOC for representative office-area and residential-area samples

The influence thresholds of different drift types on the adjustable potential of EVs are shown in Figure 4. The results indicate that stronger constraint drift continuously reduces EV adjustable potential, with voltage-related drift producing the most pronounced attenuation among the investigated cases.

The adjustable potential decreases with increasing drift intensity for all drift types, indicating a negative correlation. When the drift intensity exceeds 0.7, the adjustable potential is less than 70% of the strong impact critical value. However, the voltage surge has the most significant inhibitory effect on the adjustable potential, and it drops to less than 50% at a drift intensity of 0.5. The impact of the sudden changes in SOC is secondary, and the impact of the sharp drop in electricity prices is relatively flat. The adjustable potential is maintained above 90% in the no-drift scenario, confirming that drift is the primary factor causing the attenuation of the adjustable capability.

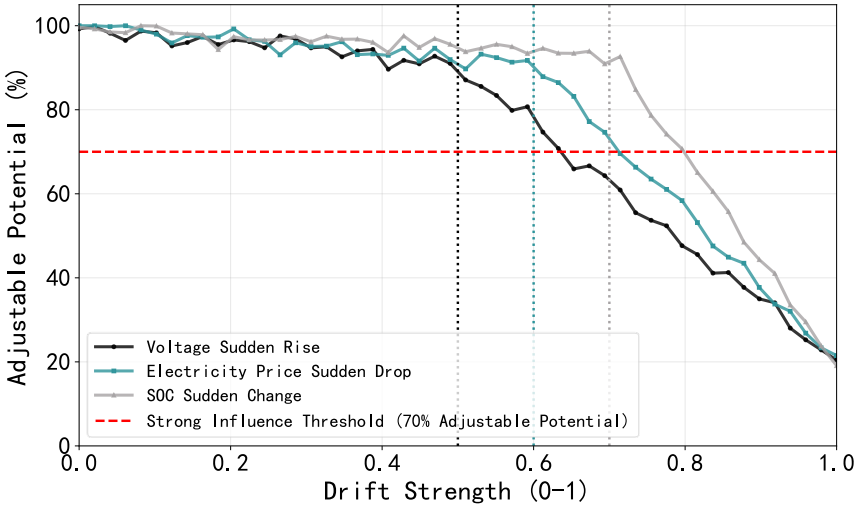


Figure 4. Relationship between adjustable potential and drift intensity

The real-time state-estimation performance and dynamic drift-tracking capability of the proposed method are shown in Figure 5. The close agreement between estimated and actual adjustable power confirms that the proposed method can rapidly track EV adjustable-capability variations even during multi-constraint drift events.

The figure includes the actual adjustable power, the online state-estimation result, and the state-estimation error band, with the drift-event period marked. During non-drift periods, the estimated adjustable power closely tracks the actual adjustable power, with the error remaining within 0.3 kW. During the drift-event period, although the actual adjustable

power fluctuates significantly due to multi-constraint interactions, the proposed method tracks these variations rapidly, with an average state-estimation error of only 0.44 kW. The narrow error band and limited response lag demonstrate the dynamic state estimation and drift-tracking capabilities of the proposed Digital Twin framework.

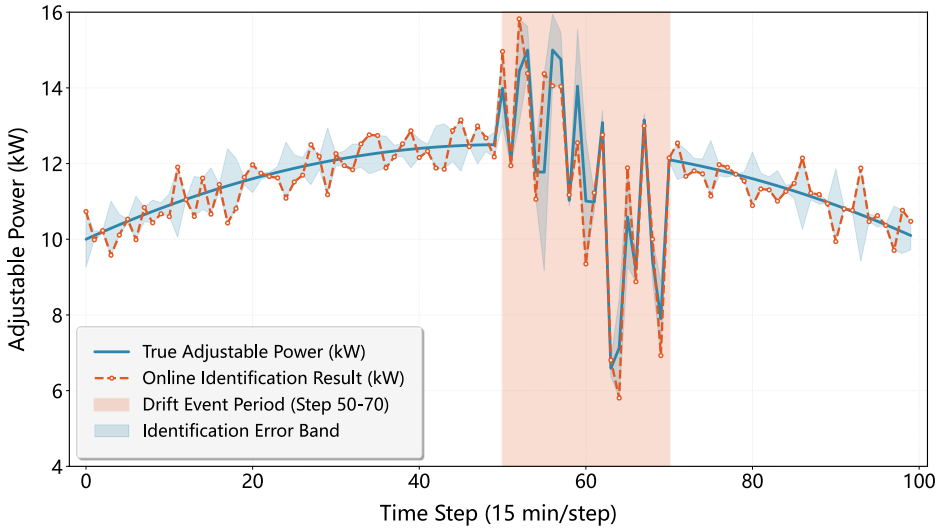


Figure 5. Real-time estimation of dynamic responses

The case study results demonstrate that the proposed Digital Twin-driven framework effectively quantifies the multidimensional coupling among grid constraints, market incentives, and EV operational states. It identifies the critical thresholds at which state drift significantly affects EV-adjustable capability and provides model–data hybrid digital-twin support for real-time distribution-network dispatch.

6. Conclusion

This study proposes a Digital Twin-driven state estimation and distributed control framework for EV adjustable capability under constraint drift. The framework integrates EV–grid–market physical modeling, a digital twin historical scenario library, twin-driven state perception, digital twin boundary evolution, and distributed control execution. Based on adaptive segmentation and hierarchical state-drift estimation, the proposed method can identify both single-constraint drift and multi-constraint interactive drift, and dynamically update EV adjustable boundaries according to drift intensity, online estimation error, and digital twin historical scenario knowledge.

Case studies using charging-pile operational data in Tianjin demonstrate that the proposed framework effectively adapts to dynamic drift scenarios and provides accurate state-estimation results for distribution-network dispatch. The proposed method quantifies the coupling relationship among grid physical constraints, market incentives, and EV operational states, tracks the attenuation of adjustable capability under state drift, and supports safe and economical operation of distribution networks.

Future work will focus on multi-regional EV cluster coordination, extreme-weather-induced changes in charging behavior, grid-fault drift, incomplete measurement conditions, and communication-delay effects. These factors will be further incorporated into the digital twin historical scenario library to improve the robustness and generalization capability of EV adjustable capability state estimation.

Acknowledgements

The work is jointly supported by State Grid Corporation of China Headquarters Science and Technology Project, Analysis of Electric Vehicle Charging/Discharging Resource Characteristics Under Multi-Factors and Interactive Guidance Technology Research & Application (5400-202412367A-3-1-KJ).

References

[1] Yousuf AKM, Wang Z, Paranjape R, et al. An in-depth exploration of electric vehicle charging station infrastructure: a comprehensive review of challenges, mitigation approaches, and optimization strategies. IEEE Access. 2024;12:51570–51589.

[2] Ma Y, Li Y, Madawala UK, et al. Integration of electric vehicle into power grid: definition, architecture and application prospect. Eng Sci Technol Int J. 2026;79:102411.

[3] Vogel-Heuser B, Ocker F, Weiß I, et al. Potential for combining semantics and data analysis in the context of digital twins. Philos Trans R Soc A Math Phys Eng Sci. 2021;379(2207):20200368.

[4] Pribiš R, Drahoš P, Kozák Š, et al. Design and validation of a flexible framework for developing generic digital twins for Industry 4.0. Sci Rep. 2025;15:44495.

[5] Do BKL, Nguyen TH, Quang NH, et al. A digital twin framework for decision-support and optimization of EV

charging infrastructure in localized urban systems. Comput Environ Urban Syst. 2026;127:102422.
[6] Al Muttaki MR, Afrin S, Anil AIA, et al. State-of-charge-aware charging opportunity detection for electric vehicles using data-driven learning and digital twin simulation. Energy Convers Manag X. 2026;30:101775.
[7] Farooq S, Harshith M, Bhatkhande A, et al. Real-time adaptive neural network-based state of charge prediction of battery pack in a digital twin framework. Array. 2026;29:100638.
[8] Abiassaf GA, Arkadan AA. Impact of EV charging, charging speed, and strategy on the distribution grid: a case study. IEEE J Emerg Sel Topics Ind Electron. 2024;5(2):531–542.
[9] Munshi A, Mohamed YARI. Extracting and defining flexibility of residential electrical vehicle charging loads. IEEE Trans Ind Inform. 2018;14(2):448–461.
[10] Sun G, Li G, Xia S, et al. ALADIN-based coordinated operation of power distribution and traffic networks with electric vehicles. IEEE Trans Ind Appl. 2020;56(5):5944–5954.
[11] Then J, Agalgaonkar AP, Muttaqi KM. Hosting capacity of an Australian low-voltage distribution network for electric vehicle adoption. IEEE Trans Ind Appl. 2024;60(2):2601–2610.
[12] Subramanian S, Gounder YK. Inter-vehicle battery charge and discharge capability assessment at EV charging station during islanded conditions in DC microgrid based on EV owner's preference. J Energy Storage. 2025;132(Part A):117673.
[13] Liu D, Zhang T, Wang W, et al. Two-stage physical economic adjustable capacity evaluation model of electric vehicles for peak shaving and valley filling auxiliary services. Sustainability. 2021;13(15):8153.
[14] Tayarani H, Tal G, Nitta CJ. Electric vehicle charging management through LSTM-based prediction of non-critical charging sessions. Transp Res Part D Transp Environ. 2026;157:105402.
[15] Wu F, Yang J, Li B, et al. Uncertain scheduling potential of charging stations under multi-attribute uncertain charging decisions of electric vehicles. Appl Energy. 2024;374:124036.
[16] Zhong YT, Gong YJ. Data-driven evolutionary computation under continuously streaming environments: a drift-aware approach. IEEE Trans Evol Comput. 2026;30(3):1210–1224.
[17] Liu C, Liu R, Liu X. A digital twin framework for intelligent electric vehicle charging optimization in smart manufacturing systems. Appl Energy. 2026;406:127281.
[18] Testasecca T, Bellesini F, Arnone D, et al. A digital twin for real-time and predictive optimization of electric vehicle charging in microgrids integrating renewable energy sources. Energies. 2025;18(21):5605.
[19] Yang Y, Han H, Shi T, et al. Study on adjustable capacity of electric vehicle charging and discharging load based on capacity reliability. Energy Technol. 2026;14(5):e70504.
[20] Basaran K, Chandrakala KRMV, Lazaroiu GC, et al. AI and digitalization in electricity markets with renewables and electric vehicles: a review of price volatility, forecasting, and stability approaches. Energy. 2026;354:141068.